



# The synthesis and characterization of lipophilic peptide-based carriers for gene delivery

Daniel J. Coles<sup>a</sup>, Anna Esposito<sup>a</sup>, Hui Ting Chuah<sup>b</sup>, Istvan Toth<sup>a,\*</sup>

<sup>a</sup>The University of Queensland, School of Chemistry and Molecular Biosciences, St Lucia, Qld 4072, Australia

<sup>b</sup>The University of Queensland, School of Pharmacy, St Lucia, Qld 4072, Australia

## ARTICLE INFO

### Article history:

Received 28 January 2010

Received in revised form 19 April 2010

Accepted 10 May 2010

Available online 13 May 2010

### Keywords:

Gene delivery

Lipid carriers

Isothermal titration calorimetry

Zetasizer

## ABSTRACT

Lipophilic carriers have shown great potential in improving the delivery of gene therapeutics. We have synthesized positively charged peptide-based carriers including lipoamino acids. The carriers were shown to interact with DNA by performing isothermal titration calorimetry and particle size and zeta potential experiments. An exothermic reaction resulted from the titration of carrier into DNA. The particle sizes of the carrier/DNA complexes varied over the different charge ratios from 200–800 nm. The zeta potential was negative at a low charge ratio but positive when the amount of carrier was increased. The utilisation of lipophilic carriers is a promising approach to improve the bioavailability of gene delivery.

© 2010 Elsevier Ltd. All rights reserved.

## 1. Introduction

Gene delivery is an exciting field of research where diseases are treated by the application of therapeutic DNA. However, despite two decades of research there is yet to be an FDA approved gene therapy drug.<sup>1</sup> The research continues as this therapy offers the only possible treatment for some diseases. The shortcomings in this field of research include DNA stability, insufficient delivery of the DNA to the target site and the toxicity or immunogenicity of the carriers employed to achieve gene delivery. Viral carriers are by far the most efficient gene delivery carriers and account for the majority of those used in clinical trials.<sup>2</sup> However, non-viral carriers are also widely studied as the immunogenicity of viral carriers can pose serious problems.<sup>3</sup> While non-viral carriers are not as efficient, they have other advantages compared to viral carriers including the ability to transfect non-dividing cells and they can deliver larger sized DNA.<sup>4</sup> Some of the most commonly used non-viral carriers include lipids, polymers, dendrimers and peptides. Lipophilicity is an important characteristic of a gene delivery carrier. It has been shown that incorporating lipophilic moieties with carriers enhances the cell uptake of DNA.<sup>5–7</sup> Cationic lipids have been used in combination with an integrin-targeting peptide and plasmid DNA. These lipopolyplexes were optimised by assessing the lipid chain length, degree of saturation and the

addition of a helper lipid.<sup>8</sup> More recently, degradable lipopolyplexes have been developed to allow the release of the complex from the endosome and subsequent release of the DNA. These complexes were found to be compact, stable and provided high transfection efficiencies.<sup>9</sup> The inclusion of lipoamino acids (LAAs) with gene delivery carriers has shown positive results for the delivery of an oligonucleotide and they have also shown the ability to protect DNA against nucleases.<sup>10–13</sup> LAAs are amino acids with a long alkyl chain. The number and chain length of the LAA can be easily changed to control the degree of lipophilicity. We have previously described the synthesis and characterization of peptide-based gene delivery carriers.<sup>14–16</sup> Here we describe the synthesis and characterization of peptide-based carriers that incorporate LAAs. The components used in our carriers are described below. Cell penetrating peptides are positively charged peptides that traverse cell membranes along with any cargo that they carry. We have used TAT (GRKKRRQRRPPQ), which is an arginine rich peptide from the HIV transcription activating factor<sup>17</sup> and penetratin (RQIKIWQNRRMKWKK), which is derived from the *Drosophila* antennapedia homeodomain transcriptional factor.<sup>18</sup> To increase the lipophilicity and stability of our gene complexes we have incorporated LAAs within our carrier. We included a nuclear localization signal (NLS) peptide (PKKKRKV), which aids in targeting the DNA to the nucleus. The NLS peptide we used is derived from the Simian virus 40 Large T antigen.<sup>19</sup> Due to previous results indicating the entrapment of our complexes inside the endosome, we also included the N-terminal of the influenza virus haemagglutinin HA2 (GLFGAIAGFIENGWEGMIDG). It causes

\* Corresponding author. Tel.: +61 7 3346 9892; fax: +61 7 3365 4273; e-mail address: [i.toth@uq.edu.au](mailto:i.toth@uq.edu.au) (I. Toth).

destabilization of the endosomal membrane at pH 5–6 due to a transformation of the peptide to a helical structure.<sup>20</sup> Lastly, we included a polylysine dendrimer with seven lysine residues to allow for an ionic interaction and condensation of the DNA. Polylysine containing eight amino acid residues is sufficient to form a complex with DNA and the lower the molecular weight, the lower the toxicity.<sup>21</sup> Polylysine is biodegradable<sup>22</sup> and the dendritic form of polylysine has been used previously for gene delivery and also included LAAs to improve the transfection efficiency.<sup>23–25</sup> We have also found that the dendritic form of polylysine containing seven lysine residues provided more effective for gene complexation and gene delivery compared to the linear form (not published). The general structure of the synthesized carriers is shown in Figure 1. Table 1 shows the peptide components used to make each carrier. Figure 2 shows the complete structure of carrier 1. These carriers were compared to previously described carriers without LAAs for their ability to form complexes with DNA by isothermal titration calorimetry (ITC) and particle size and zeta potential experiments.



Figure 1. General structure of carriers 1–6.

Table 1  
Components used for carriers in Figure 1

Carrier	U	V	W	X	Y	Z
1	C <sub>12</sub>	Lys–(Lys) <sub>2</sub> –(Lys) <sub>4</sub>	Lys	NLS	Lys	TAT
2	—	—	2C <sub>12</sub>	NLS	Lys	TAT
3	—	—	—	Lys–(Lys) <sub>2</sub> –2TAT	2C <sub>12</sub>	NLS
4	—	—	—	Lys–(Lys) <sub>2</sub> –(Lys) <sub>4</sub> –4TAT	2C <sub>12</sub>	NLS
5	C <sub>14</sub>	Lys–(Lys) <sub>2</sub> –(Lys) <sub>4</sub>	Lys	HA2	Lys	TAT
6	—	—	—	Lys–(Lys) <sub>2</sub> –(Lys) <sub>4</sub>	2C <sub>8</sub>	PEN

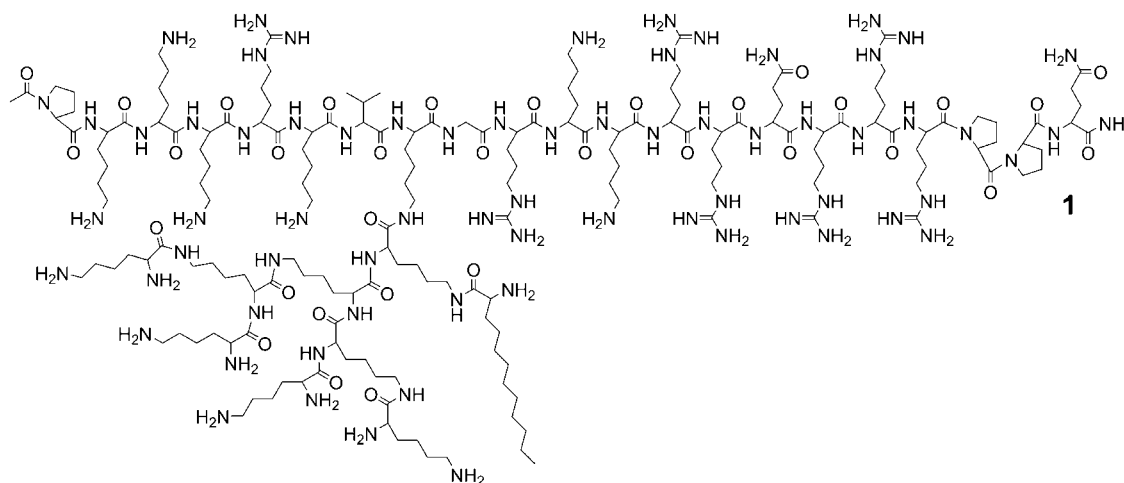


Figure 2. Complete structure of carrier 1.

## 2. Results and discussion

### 2.1. Synthesis of the gene delivery carriers

Carriers 1–6 were successfully synthesized by solid phase peptide synthesis. Different combinations of the cell penetrating peptides TAT or penetratin, a NLS peptide, a fusogenic peptide HA2, dendritic polylysine and LAAs were used to synthesize the carriers shown in Figure 1. Multiple copies of the TAT peptide were used in carriers 3 and 4 to enhance the cellular uptake of DNA. To incorporate multiple peptides into a single carrier an orthogonal

protection group strategy was used. We used lysine protected with Boc and Fmoc. Boc and Fmoc protecting groups were chosen because Boc is cleaved under acidic conditions while Fmoc is cleaved under basic conditions. Furthermore, Boc and Fmoc amino acids are readily available. A scheme for the synthesis of carrier 1 is shown in Figure 3. After their synthesis, carriers 1–6 were cleaved from the resin, purified by preparative HPLC and analysed by analytical HPLC and electro-spray mass spectrometry (ES-MS).

### 2.2. Isothermal titration calorimetry

The titration of carriers 1–6 into salmon testes DNA resulted in an exothermic reaction from the ionic interaction between the two oppositely charged entities (Fig. 4 upper panel). This was followed by an endothermic reaction, which occurred due to the precipitation of the complex. The remaining injections are heats of dilution. The exothermic interaction between carriers 2–4 with DNA was much less apparent, which was shown by the very small peaks in the raw data graph (see Supplementary data). This indicated that the other carriers, which contained a dendritic polylysine entity played a major role in the interaction with DNA. This was also shown on the raw data graph by the presence of larger defined peaks. The heat of reaction from the titration is similar to that previously described using charged peptide-based carriers without LAAs.<sup>15</sup> When examining PEI/DNA complex formation by ITC, Choosakoonkriang et al. also reported that aggregation of the complexes occurred.<sup>26</sup> A blank titration was performed where the carrier was titrated into buffer (data not shown). The heats generated from these experiments were subtracted from the Experimental data. The heat of reaction was plotted against the molar ratio (Fig. 4 bottom panel). The data was analysed using a two set of sites binding model from which a curve was fit to the data and the thermodynamic parameters for the reaction were calculated

(Table 2). The thermodynamic parameters that are shown in Table 2 for carriers 2–4 are far less accurate because the fitting procedure was more difficult and several data points were removed prior to fitting to ensure that the curve-fitting program proceeded.

The binding interaction between carriers 1–6 and DNA was strong, with the binding affinity ranging from  $2.9\text{E}+08\text{ M}^{-1}$  for carrier 6 to  $7.6\text{E}+11\text{ M}^{-1}$  for carrier 2. The high binding affinity for carrier 2 was most likely due to the difficulty experienced in the curve fitting procedure as the data points did not allow for a smooth curve and therefore the binding affinity was higher than anticipated. The precipitation of the carrier/DNA was much weaker

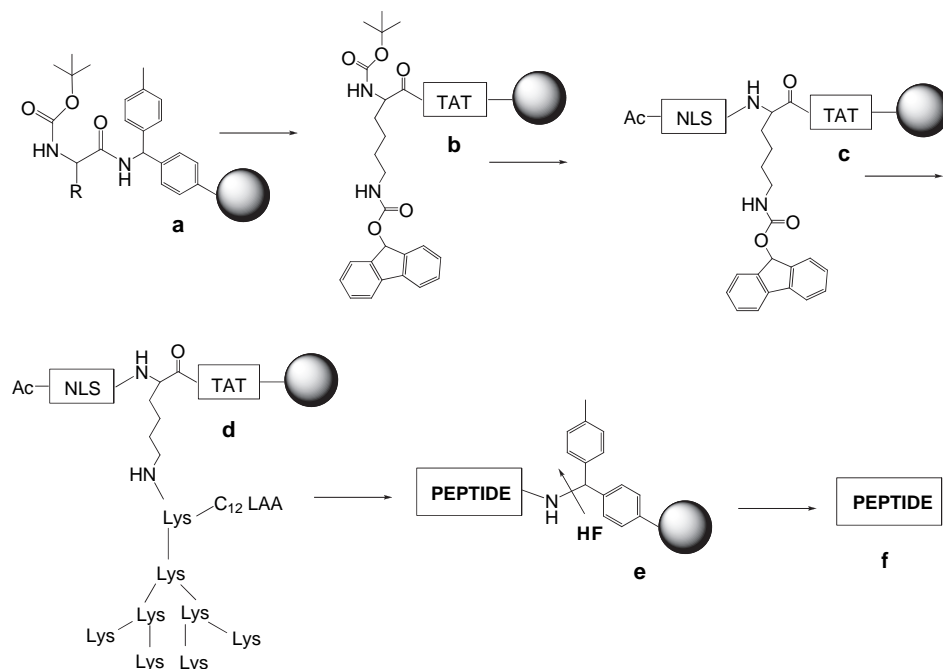


**Figure 3.** Scheme for the synthesis of carrier 1. (a) coupling of first amino acid to MBHA resin. (b) after the TAT peptide was completed, Boc–Lys(Fmoc) was coupled. (c) The Boc group was removed followed by coupling of the NLS peptide and N-terminal acetylation. (d) The Fmoc group was removed followed by coupling Boc–Lys(Fmoc), removal of Boc group, coupling of polylysine dendrimer, removal of Fmoc group and coupling of C<sub>12</sub> LAA. (e) HF cleavage of the peptide from the MBHA resin. (f) peptide product.

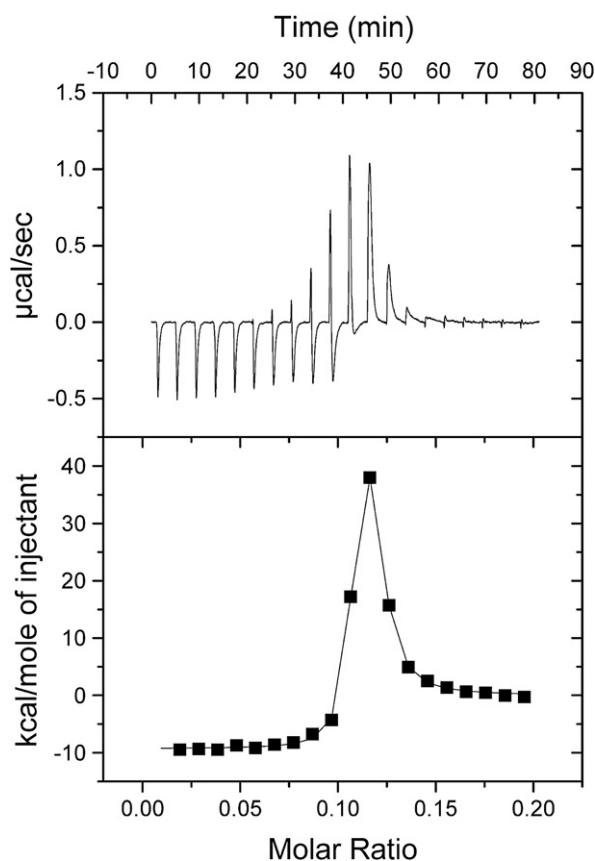


**Figure 4.** Isothermal titration calorimetry graph for the titration of carrier 1 into DNA. The top panel represents the power change to the sample cell upon the addition of carrier 1 into DNA. The bottom panel represents the integrated area of the peaks from the top panel, which is plotted against the molar ratio.

with a binding affinity of  $4.7\text{E}+06\text{ M}^{-1}$  for carrier 6 to  $5.8\text{E}+07\text{ M}^{-1}$  for carrier 3. The enthalpy of the binding reaction resulted in a larger negative value for the carriers containing dendritic polylysine (carriers 1 and 5–7). This was due to much more heat being released from their interaction with the DNA. The entropy was positive for both processes and was much larger for the precipitation reaction. The entropy of the binding reaction was larger for the carriers without dendritic polylysine (carriers 2–4). The calculation of Gibbs free energy showed that both processes are spontaneous since they are negative values. Gibbs free energy is also correlated to the binding affinity with a higher binding affinity resulting in a larger negative value. The charge ratio of carrier/DNA at the stoichiometric point of the binding between the carriers and DNA was about 1:1 for all carriers. The results generated from these titrations show similar characteristics compared to compounds we have previously published.<sup>15</sup> When comparing the results of carriers 1–6 with the same carriers but with no LAAs those carriers had a slightly lower binding affinity and enthalpy. We have previously worked with LAA/polylysine carriers to enable oligonucleotide delivery. The titration of such carriers into an oligonucleotide resulted in an exothermic reaction.<sup>11</sup> However, there was no precipitation of the complex. In this study we also examined one of these previously described carriers containing two C<sub>14</sub> LAAs and a polylysine dendrimer (carrier 7). Titrating carrier 7 into salmon testes DNA resulted in the same type of interaction as the other carriers. However, the binding affinity and enthalpy was the lowest of any carrier (Table 3). Carrier 7 has eight positive charges, which is much lower than all other carriers examined in this study. Therefore, the number and composition of the positive charges in the carriers clearly had an impact on the thermodynamics of the interaction with DNA.

The energy required to condense DNA is quite large. However, the ability of DNA to condense into a compact particle by using polycationic compounds with as little as three positive charges has been reported.<sup>27</sup> The reversibility of the condensation process is dependent upon the amount of ligand used when condensing the DNA.<sup>27</sup> Condensed DNA can form toroids due to the stiffness, low attractive forces and concentration of DNA but it is also dependent

**Table 2**  
Thermodynamic parameters from the titration of carriers **1–7** into DNA

Carrier	Binding affinity (M <sup>-1</sup> )		Enthalpy (kcal/mol)		Entropy (kcal/mol)		Gibbs free energy (kcal/mol)		Stoichiometry	
	K <sub>a1</sub>	K <sub>a2</sub>	ΔH1	ΔH2	ΔS1	ΔS2	ΔG1	ΔG2	n1	n2
1	6.9E+08	7.4E+06	−9.7	80.4	0.008	0.301	−12.1	−9.4	0.107	0.012
2	7.6E+11	3.9E+07	−0.5	12.3	0.053	0.076	−16.1	−10.3	0.149	0.017
3	9.9E+09	5.8E+07	−3.4	35.8	0.034	0.155	−13.5	−10.4	0.078	0.008
4	6.8E+11	4.0E+07	−5.4	41.4	0.036	0.207	−16.1	−10.4	0.051	0.010
5	3.3E+09	1.1E+07	−11.7	28.0	0.004	0.126	−12.9	−9.6	0.162	0.028
6	2.9E+08	4.7E+06	−10.2	32.6	0.004	0.140	−11.5	−9.1	0.145	0.027
7	1.1E+08	1.6E+06	−8.4	24.5	0.008	0.110	−10.8	−8.5	0.329	0.049

upon the type of DNA used.<sup>27</sup> The reduction in the size of the DNA is influenced by hydration, electrostatic interactions and hydrophobicity. The binding of polycations to the phosphate backbone of DNA was reported to be entropically driven by the release of water.<sup>28,29</sup> However, it was also reported to be enthalpically driven for the interaction between a polymer and DNA.<sup>30</sup> Furthermore, the inclusion of lipids with polycations enhances the binding cooperativity by inhibiting water molecules around the DNA.<sup>28</sup> The interaction between positively charged carriers and negatively charged DNA also have a contribution from the release of the associated counter ions.<sup>31</sup> Other cationic carriers such as spermidine and cobalt hexammine have shown the ability to bind to DNA. However, their interaction was endothermic.<sup>32,33</sup> The ability of the cell penetrating peptide TAT to bind with DNA from salmon testes has been reported.<sup>34</sup> Compared to our system, which contained many cell penetrating peptides in combination with LAAs both still resulted in an exothermic reaction. However, Ziegler et al. reported no precipitation of their complexes.<sup>34</sup> It has been demonstrated previously that the binding between cationic lipids and DNA was endothermic.<sup>35</sup> On the contrary, we have shown an exothermic interaction between our cationic lipid carriers and DNA. We have also shown that the composition of the charged peptides within the carrier played a significant role in determining the thermodynamic parameters of the reaction. When polylysine dendrimers were included within the carrier we observed a more significant response when they were titrated into DNA.

### 2.3. Particle size and zeta potential

The particle size and zeta potential of the carrier/DNA complexes are important factors to determine to enable the successful

**Table 3**  
Analytical data of the purified carriers **1–6**

Carrier	MW	ES-MS ( <i>m/z</i> )	Retention time (min) <sup>a</sup>	Retention time (min) <sup>b</sup>
1	3977.04	1327.1 ( <i>z</i> =3) 995.5 ( <i>z</i> =4) 797.0 ( <i>z</i> =5)	12.23	8.40
2	3105.96	1554.4 ( <i>z</i> =2) 1036.7 ( <i>z</i> =3) 777.8 ( <i>z</i> =4)	16.72	15.90, 16.13
3	5063.30	1689.7 ( <i>z</i> =3) 1267.4 ( <i>z</i> =4) 1014.3 ( <i>z</i> =5)	15.26	15.19, 16.37
4	8977.99	1498.5 ( <i>z</i> =6) 1284.2 ( <i>z</i> =7) 1123.8 ( <i>z</i> =8)	13.69	10.28, 11.29
5	5175.25	1727.0 ( <i>z</i> =3) 1295.4 ( <i>z</i> =4) 1036.8 ( <i>z</i> =5)	19.08	16.68
6	3425.37	1714.0 ( <i>z</i> =2) 1143.4 ( <i>z</i> =3) 857.6 ( <i>z</i> =4)	14.96, 15.68	18.27, 19.43 <sup>c</sup>

<sup>a</sup> Solvent B1.

<sup>b</sup> solvent B2.

<sup>c</sup> Methanol was used in solvent B2 for carrier **6**.

delivery of the DNA to the target cells. DNA is a large negatively charged hydrophilic molecule, which does not diffuse through cell membranes. The particle size (*z*-average) and zeta potential (particle charge) of the carrier/gene complexes were assessed at five different charge ratios (+/−) (Fig. 5). At all charge ratios the size of the complexes varied from 200–800 nm in diameter. It was interesting to see that lowest *z*-averages observed occurred when the charge ratio was lower. In contrast, our previous experiments with peptides without LAAs had shown that the higher the charge ratio, the smaller the particle size.<sup>14</sup> The zeta potential at a charge ratio of 0.5:1 (+/−) was slightly negative as there was insufficient carrier present to neutralize the DNA. However, as the charge ratio was increased the zeta potential of the particles increased to be positive as there was an excess of the positively charged carrier. This trend was also observed in our previous study.<sup>14</sup>

Carrier **7** showed a similar profile compared to the other carriers except that the zeta potential was negative at a 1:1 charge ratio compared to all other carriers where it was positive. The reason may be that carrier **7** only contains eight positive charges. The zeta potential at the 1:1 charge ratio resulted in a larger positive number for the carriers containing more positive charges. There was no observable difference in the pattern observed for the particle size and zeta potential results compared to the ITC results where the binding reaction was much less apparent for carriers **2–4**. The complexes obtained were much larger compared to our previously obtained results (carriers without LAAs). The LAAs could hinder the collapse of the DNA due to the hydrophobic effect. This effect occurs due to the inclusion of long acyl chains in the carrier, which then stop the DNA from condensing into a tight package.<sup>28</sup> There are many factors, which could affect the formation of polycations/DNA particles including salt concentration, pH and temperature. In these experiments the pH of the buffer used was 7.2, whereas the pH of the buffer used for the experiments in our previous paper was 3.2.<sup>15</sup> Therefore, having a lower pH increases the ability of the carrier to compact the DNA or less DNA and carrier is contained within a single particle. There was a 5 to 10 fold increase in the size of the carriers in the current study compared to the previously examined carriers. To test if the larger particle size was due to the pH or the presence of LAAs in the carrier, carrier **6** was assessed at pH 3.2. The particle size was found to be around 80–100 nm for all charge ratios (see [Supplementary data](#)) compared to the experiment reported here where the particle size ranged from 200–600 nm (Fig. 5f).

### 3. Conclusion

Using lipophilic carriers may provide a means to overcome some of the significant barriers associated with gene delivery. We have shown that incorporating LAAs with peptides had no effect on the formation of the carrier/gene complexes when assessed by ITC and zetasizer. The binding affinity with DNA was found to be higher for the carriers, which have a higher number of positive charges. We have also shown that the dendritic polylysine component was the

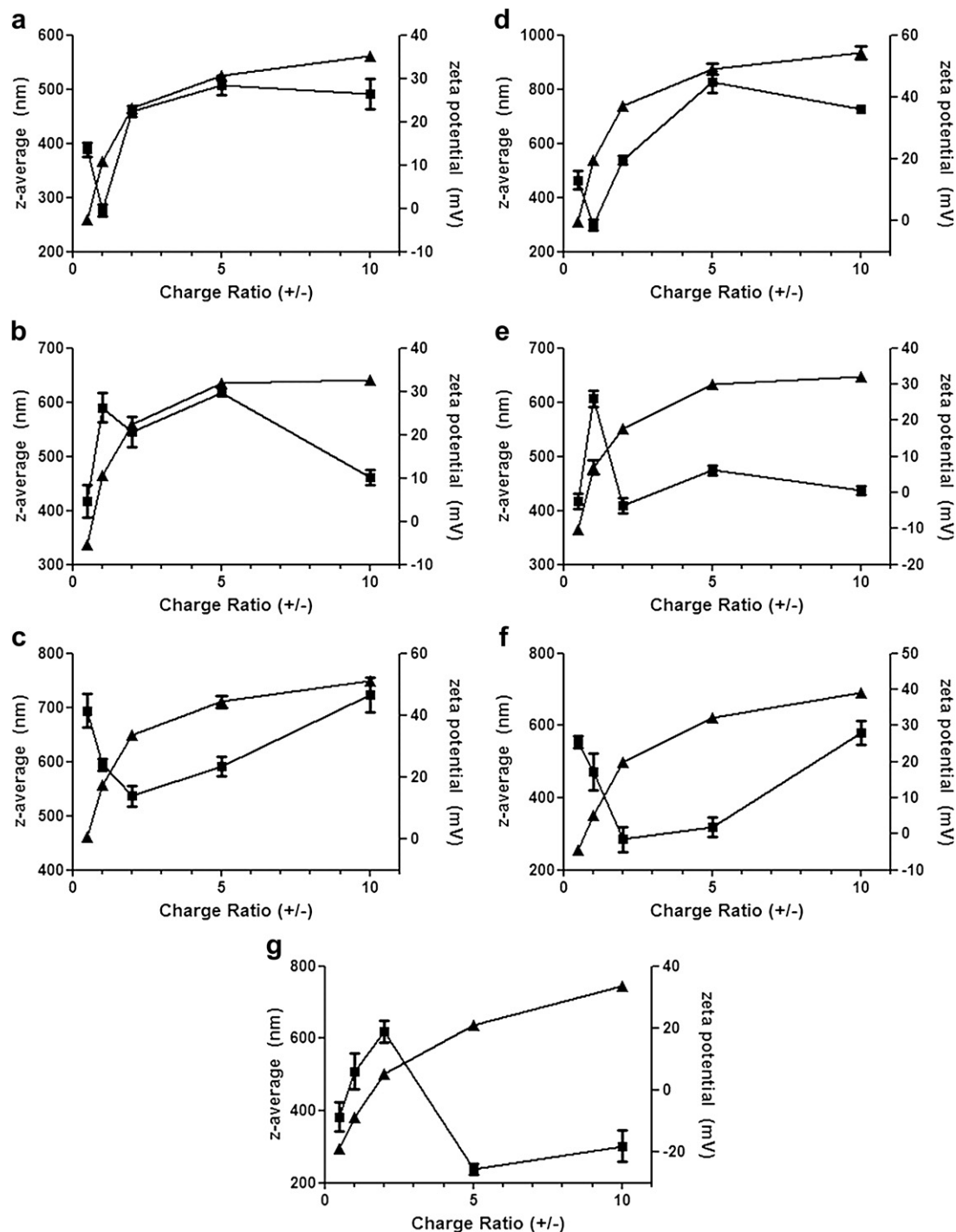


**Figure 5.** Particle size (z-average) and zeta potential of carrier/pGL3 DNA complexes. pGL3 DNA complexed with carrier (a) 1, (b) 2, (c) 3, (d) 4, (e) 5, (f) 6, (g) 7. Measurements were conducted at five different charge ratios (+/-). Square (■) indicates z-average (left axis) and triangle (▲) indicates zeta potential (right axis). All data presented as mean±s.e.m,  $n=3$ .

major contributing factor in the binding process with DNA. The experimental conditions are also an essential factor in the carrier/DNA complex formation process.

#### 4. Experimental

##### 4.1. Materials

*p*-4-Methyl benzhydryl amine (MBHA) resin and Boc-L-amino acids were purchased from NovaBiochem (Switzerland), GL Biochem (Shanghai, China) or Reanal (Budapest, Hungary). Peptide

synthesis grade dimethylformamide (DMF), trifluoroacetic acid (TFA), *N,N*-diisopropylethylamine (DIPEA) and 2-(1*H*-benzotriazol-1-yl)-1,1,3,3-tetramethyluronium hexafluorophosphate (HBTU) were purchased from Auspep (Melbourne, Australia). HPLC grade acetonitrile (ACN), Isopropanol (IP) and methanol (MeOH) were purchased from Labscan Asia Co. Ltd (Bangkok, Thailand) or Honeywell-Burdick & Jackson (Morristown, NJ). DNA from salmon testes (double-stranded) and all other reagents were purchased from Sigma Aldrich (Castle Hill, Australia) at the highest available purity. pGL3 DNA was amplified and purified according to the manufacturers protocol (Invitrogen).



## 4.2. Synthesis of lipoamino acids

LAAs consisting of 8, 12 and 14 carbon atoms were synthesized according to previously described methods.<sup>36</sup> They were subsequently Boc-protected to facilitate their use in solid phase peptide synthesis.<sup>36</sup>

## 4.3. General procedure for the synthesis of carriers 1–6

Carriers **1–6** were synthesized by solid phase peptide synthesis using Boc chemistry.<sup>37</sup> *p*-MBHA resin (100–200 mesh, 0.31 mmol/g or 0.4 mmol/g loading) was swollen in DMF in a sintered glass peptide synthesis vessel for 1 h. Each Boc-L-amino acid (4 equiv) was activated in a mixture of HBTU (0.5 M in DMF, 4 equiv) and DIPEA (6 equiv) then mixed with the resin for 30 min. Coupling efficiency was monitored using the negative ninhydrin reaction (5 min). Coupling was considered successful if greater than 99.6% otherwise the coupling procedure was repeated. The Boc-protecting group was removed using neat TFA (2×1 min) followed by in situ neutralisation. Side chain protecting groups used include Lys (2-Cl-Z), Lys(Fmoc), Arg(Tos), Trp(For) and Gln(Xan). Between all manipulations, the resin was washed thoroughly with DMF. Carriers **1**, **2** and **5** were synthesized by using an orthogonal protection group strategy. Boc–Lys(Fmoc) was coupled after the TAT peptide. *N*<sup>2</sup>-Boc was removed, followed by the coupling of the NLS or HA2 peptide in a stepwise fashion. The N-terminus was acetylated by treating the resin with acetic anhydride (1 mL), DIPEA (0.5 mL) and DMF (10 mL) twice for 30 min. With the N-terminal protected, lysine *N*<sup>6</sup>-Fmoc deprotection was performed using 20% piperidine in DMF (5 min and 20 min). For carrier **2**, two C<sub>12</sub> LAAs were then coupled to the peptide. For carriers **1** and **5** Boc–Lys(Fmoc) was coupled to the peptide followed by Boc deprotection. Boc–Lys(Boc) was then coupled to the peptide until the polylysine dendrimer was complete. While leaving the polylysine dendrimer Boc-protected, lysine *N*<sup>6</sup>-Fmoc deprotection was performed followed by coupling of the LAA. For carriers **3** and **4** Boc–Lys(Fmoc) was used in the last coupling procedure for the polylysine scaffold. After Boc deprotection the TAT peptide was coupled in a stepwise fashion, followed by lysine *N*<sup>6</sup>-Fmoc deprotection. Upon completion of the carriers, the terminal Boc-protecting groups were removed and the resin washed exhaustively with DMF, dichloromethane and methanol. The resin was dried over KOH under vacuum. The carriers were cleaved from the resin using hydrogen fluoride (10 mL/g resin) and *p*-cresol (10%) or *p*-cresol (5%) and *p*-thiocresol (5%) at 0 °C for 2 h. The cleaved carriers were precipitated in diethyl ether, then redissolved in 50% ACN and lyophilised to give a white amorphous powder. The synthesis of carrier **7** has been described previously.<sup>10</sup>

## 4.4. Purification

Firstly, the carriers were analysed using analytical reverse phase-high performance liquid chromatography (RP-HPLC) on a Shimadzu instrument (LC-10AT liquid chromatograph, SCL-10A system controller, SPD-6A UV detector, a SIL-6B auto injector with a SCL-6B system controller and column C4 (Vydac, 3.5 μm pore size, id=4.6, 150 mm)) to identify their retention time and to establish a purification method. Preparative HPLC was undertaken on a Waters HPLC system (Model 600 controller, 490E UV detector, F pump and TSK Gel C4 column with 10 μm pore size and 22 mm id) with 100 mg of crude dendrimer. They were separated using a gradient of solvent A (0.1% TFA/H<sub>2</sub>O) and solvent B (90% ACN/0.1% TFA/H<sub>2</sub>O) and the fractions collected were characterized by electro-spray mass spectrometry (ES-MS) (Perkin–Elmer API 3000 instrument). The pure fractions were added together and lyophilised. The purified carriers were analysed by ES-MS and analytical RP-HPLC using solvent A (0.1% TFA/H<sub>2</sub>O) and either solvent B1 (90% ACN/0.1% TFA/

H<sub>2</sub>O) or solvent B2 (90% Isopropanol/0.1% TFA/H<sub>2</sub>O) using a gradient of 0–100% B over 30 min (Table 3).

## 4.5. Isothermal titration calorimetry

Isothermal titration calorimetry (ITC) was performed using a MicroCal VP-ITC Microcalorimeter (Northampton, MA, USA) with Origin 5.0 software and VPViewer 2000. In all titrations the solvent used was 20 mM Hepes buffer (pH 7.2). The concentration of DNA in base pairs (bp) was determined spectrophotometrically<sup>34</sup> at 260 nm using an extinction coefficient of 13,200 M (bp)<sup>−1</sup> cm<sup>−1</sup>. The micro-syringe contained the carrier (2 mg/mL), the sample cell contained salmon testes DNA (0.1 mM (bp)) and the reference cell contained buffer. Before measurements were taken, all solutions were degassed. Each injection (3 μL for **1–4** and **7**, 5 μL for **5** and 4 μL for **6**) was 4 min apart and the experiment was performed at a constant temperature of 25 °C. The thermodynamic parameters were calculated by averaging two separate experimental results.

## 4.6. Particle size and zeta potential

A Zetasizer Nano ZP instrument (Malvern Instruments, UK) with DTS software was used for particle size and zeta potential measurements of the dendrimer/pGL3 DNA complexes. Sizes were analysed using a non-invasive back scatter system and zeta potentials were measured using M3-PALS technique. Measurements were taken at 25 °C with scattering angle of 173° using disposable capillary cuvettes. Complexes were prepared by diluting various amounts of dendrimer with 500 μL of 20 mM Hepes buffer (pH 7.2) and adding drop wise to 2 μg pGL3 DNA in 500 μL of 20 mM Hepes buffer (pH 7.2). The solution was vortexed and left for 60 min prior to analysis. The experiments were performed in triplicate and used five different charge ratios (+/−).

## Acknowledgements

The authors thank Mr. Makan Khoshnejad for the preparation of the pGL3 DNA.

## Supplementary data

Supplementary data associated with this article can be found, in the online version, at doi:10.1016/j.tet.2010.05.031. These data include MOL files and InChIKeys of the most important compounds described in this article.

## References and notes

- Gene Therapy, U.S. DOE Human Genome Project; <http://www.ornl.gov/hgmis/home.shtml> (accessed 28/01/10).
- Edelstein, M. L.; Abedi, M. R.; Wixon, J. J. *Gene Med.* **2007**, *9*, 833–842.
- Verma, I. M.; Weitzman, M. D. *Annu. Rev. Biochem.* **2005**, *74*, 711–738.
- Lee, M.; Kim, S. W. *Pharm. Res.* **2005**, *22*, 1–10.
- Prata, C. A. H.; Zhang, X. X.; Luo, D.; McIntosh, T. J.; Barthelmy, P.; Grinstaff, M. W. *Bioconjugate Chem.* **2008**, *19*, 418–420.
- Li, W. J.; Szoka, F. C. *Pharm. Res.* **2007**, *24*, 438–449.
- Schroeder, A.; Levins, C. G.; Cortez, C.; Langer, R.; Anderson, D. G. *J. Intern. Med.* **2010**, *267*, 9–21.
- Writer, M.; Hurley, C. A.; Sarkar, S.; Copeman, D. M.; Wong, J. B.; Odlyha, M.; Lawrence, M. J.; Tabor, A. B.; McAnulty, R. J.; Shamlou, P. A.; Hailes, H. C.; Hart, S. L. *J. Liposome Res.* **2006**, *16*, 373–389.
- Mustapa, M. F. M.; Grosse, S. M.; Kudsiova, L.; Elbs, M.; Raiber, E. A.; Wong, J. B.; Brain, A. P. R.; Armer, H. E. J.; Warley, A.; Keppler, M.; Ng, T.; Lawrence, M. J.; Hart, S. L.; Hailes, H. C.; Tabor, A. B. *Bioconjugate Chem.* **2009**, *20*, 518–532.
- Wimmer, N.; Marano, R. J.; Kearns, P. S.; Rakoczy, E. P.; Toth, I. *Bioorg. Med. Chem. Lett.* **2002**, *12*, 2635–2637.
- Marano, R. J.; Wimmer, N.; Kearns, P. S.; Thomas, B. G.; Toth, I.; Brankov, M.; Rakoczy, P. E. *Exp. Eye Res.* **2004**, *79*, 525–535.
- Marano, R. J.; Toth, I.; Wimmer, N.; Brankov, M.; Rakoczy, P. E. *Gene Ther.* **2005**, *12*, 1544–1550.

13. Parekh, H. S.; Marano, R. J.; Rakoczy, E. P.; Blanchfield, J.; Toth, I. *Bioorg. Med. Chem.* **2006**, *14*, 4775–4780.
14. Coles, D. J.; Yang, S.; Esposito, A.; Mitchell, D.; Minchin, R. F.; Toth, I. *Tetrahedron* **2007**, *63*, 12207–12214.
15. Coles, D. J.; Yang, S.; Minchin, R. F.; Toth, I. *Biopolymers* **2008**, *90*, 651–654.
16. Yang, S.; Coles, D. J.; Esposito, A.; Mitchell, D. J.; Toth, I.; Minchin, R. F. *J. Controlled Release* **2009**, *135*, 159–165.
17. Deshayes, S.; Morris, M. C.; Divita, G.; Heitz, F. *Cell. Mol. Life Sci.* **2005**, *62*, 1839–1849.
18. Kerkis, A.; Hayashi, M. A. F.; Yamane, T.; Kerkis, I. *Iubmb Life* **2006**, *58*, 7–13.
19. Vaysse, L.; Gregory, L. G.; Harbottle, R. P.; Perouzel, E.; Tolmachov, O.; Coutelle, C. *J. Gene Med.* **2006**, *8*, 754–763.
20. Cho, Y. W.; Kim, J. D.; Park, K. J. *Pharm. Pharmacol.* **2003**, *55*, 721–734.
21. Kiselev, A. V.; Il'ina, P. L.; Egorova, A. A.; Baranov, A. N.; Guryanov, I. A.; Bayanova, N. V.; Tarasenko, I. I.; Lesina, E. A.; Vlasov, G. P.; Baranov, V. S. *Russ. J. Genet.* **2007**, *43*, 593–600.
22. Boyd, B. J.; Kaminskas, L. M.; Karellas, P.; Krippner, G.; Lessene, R.; Porter, C. J. H. *Mol. Pharmacol.* **2006**, *3*, 614–627.
23. Toth, I.; Sakthivel, T.; Wilderspin, A. F.; Bayele, H.; O'Donnell, M.; Perry, D. J.; Pasi, K. J.; Lee, C. A.; Florence, A. T. *STP Pharma Sci.* **1999**, *9*, 93–99.
24. Shah, D. S.; Sakthivel, T.; Toth, I.; Florence, A. T.; Wilderspin, A. F. *Int. J. Pharm.* **2000**, *208*, 41–48.
25. Bayele, H. K.; Sakthivel, T.; O'Donnell, M.; Pasi, K. J.; Wilderspin, A. F.; Lee, C. A.; Toth, I.; Florence, A. T. *J. Pharm. Sci.* **2005**, *94*, 446–457.
26. Choosakoonkriang, S.; Lobo, B. A.; Koe, G. S.; Koe, J. G.; Middaugh, C. R. *J. Pharm. Sci.* **2003**, *92*, 1710–1722.
27. Bloomfield, V. A. *Biopolymers* **1997**, *44*, 269–282.
28. Patel, M. M.; Anchordoquy, T. J. *Biophys. J.* **2005**, *88*, 566A–567A.
29. Bronich, T.; Kabanov, A. V.; Marky, L. A. *J. Phys. Chem. B* **2001**, *105*, 6042–6050.
30. Tan, J. F.; Too, H. P.; Hatton, T. A.; Tam, K. C. *Langmuir* **2006**, *22*, 3744–3750.
31. Meier-Koll, A. A.; Fleck, C. C.; von Grunberg, H. H. *J. Phys.: Condens. Matter* **2004**, *16*, 6041–6052.
32. Matulis, D.; Rouzina, I.; Bloomfield, V. A. *J. Mol. Biol.* **2000**, *296*, 1053–1063.
33. Kim, W.; Yamasaki, Y.; Kataoka, K. *J. Phys. Chem. B* **2006**, *110*, 10919–10925.
34. Ziegler, A.; Seelig, J. *Biochemistry* **2007**, *46*, 8138–8145.
35. Pozharski, E.; MacDonald, R. C. *Biophys. J.* **2003**, *85*, 3969–3978.
36. Gibbons, W. A.; Hughes, R. A.; Charalambous, M.; Christodoulou, M.; Szeto, A.; Aulabaugh, A. E.; Mascagni, P.; Toth, I. *Liebigs Ann. Chem.* **1990**, 1175–1183.
37. Schnolzer, M.; Alewood, P.; Jones, A.; Alewood, D.; Kent, S. B. H. *Int. J. Pept. Protein Res.* **1992**, *40*, 180–193.